FUDMA Journal of Engineering and Technology
ISSN: 3092-9385
https://fjet.fudutsinma.edu.ng/index.php/fjet/
Volume 2, Issue 2, 2026, 124-135

Experimental and Finite Element Investigation of Thermal Distribution and Heat Flux in an Internal Combustion Engine Cylinder

Sunday IWERIOLOR[1*], Ngozi G. EMORDI[2], Festus O. ISAAC[3], Linus CHUKWUKA[4], Onyekachukwu N. AKPENYI-ABOH[5], Liberty ANWULE[6]

[1*,4,5,6]Department of Mechanical Engineering, Faculty of Engineering, University of Delta, Agbor, Delta State, Nigeria
[2]Department of Mechatronics Engineering, Faculty of Engineering, University of Delta, Agbor, Delta State, Nigeria
[3]Department of Mechanical Engineering, Faculty of Engineering, Edo state University, Iyahmo, Edo State, Nigeria

[1*]sunday.iweriolor@unidel.edu.ng, [2]ngozi.emordi@unidel.edu.ng, [3]isaac.oamen@edouniversity.edu.ng, [4]linus.chukwuka@unidel.edu.ng, [5]onyekachukwu.akpenyi-aboh@unidel.edu.ng, [6]liberty.anwule@unidel.edu.ng

Abstract
The radial temperature variation, heat flow, heat-transfer rate, and convective cooling pattern within an engine cylinder wall were all examined using experimental and finite-element methods. At particular points along the cylinder wall, radial temperature measurements were taken from the inner combustion surface. The simulated temperatures resulting from steady-state finite-element thermal analysis were compared with experimental data. Experimented temperature data displayed a steady temperature drop from 450 °C at the inner wall to 158 °C at the exterior wall. Errors margins of 0.50 °C, 11.48 °C, and 3.13 °C were observed as simulated temperatures nearly approximate to interpolated experimental data. A maximum total heat flow of 5.415 × 10² W/m² became apparent via Temperature Contour analysis, resulting to a simulated heat-transfer rate of 146 kW.This is consistent with the experimental figure of 147 kW (0.68% deviation). The experimental result of 1100 W/m²•K differs 1.8% from the estimated convective heat-transfer coefficient of 1080 W/m²•K. The remarkable correlation between the observed and simulated temperatures, heat flux, heat-transfer rate, and convective coefficient indicates that the well-established finite-element framework provides a reliable and experimentally validated technique for quantifying heat transfer in engine cylinders. This provides a strong basis for the development of improved coatings, high-temperature-resistant materials, and cooling techniques in the future as well as a verifiable technique for establishing engine cylinder performance, durability, and thermal variables.

Keywords: *Thermal Analysis, Engine Cylinder, Temperature, Finite Element, Heat transfer.*

1.0 Introduction

Internal combustion engines (ICEs) are required to undergo thermal assessment to improve performance, longevity, and pollution standard adherence. [1]. Complex thermal loads from high-temperature gases and frictional heating affect engine components [2,3,4]. The assessment of temperature distributions is simplified by a steady-state thermal analysis [5]. Heat dissipation can be maximized while following the equation for steady-state heat conduction [6, 7]. Highly precise characterization of heat transport processes is feasible by the incorporation of cylindrical coordinate systems in thermal modeling, which is consistent with the rotating geometry of engine cylinder [8,9, 10].

Engineers may quickly identify thermal bottlenecks and evaluate cooling strategies with this method. [11.12 ,13]. The unique form of engine cylinders adds complexity to thermal modeling because Cartesian coordinates typically conflict with their radial and circumferential symmetry. This misalignment might lead to numerical inaccuracies and complicate boundary conditions [14.15]. Errors in cylinder liner models have been attributed to neglecting temperature-dependent material properties [16, 17, and 18]. Moreover, asymmetric heat loads from uneven fuel injection or coolant flow necessitate more sophisticated models to account for temperature variations [19].

The thermal behavior of engine cylinders and associated parts under real combustion and transient running circumstances has been studied. However, complicated combustion processes, varying engine loads, transient boundary conditions, and advanced heat-flux measuring devices are frequently included in these investigations. Isolating the basic mechanisms controlling radial heat conduction through the cylinder wall becomes challenging under such circumstances [20] Therefore, an effective approach for investigating the underlying heat-transfer behavior is a controlled laboratory-scale experimental method that can replicate the crucial thermal boundary conditions of an engine cylinder In an effort to demonstrate how the temperature field varies across the liner under various engine loads and speeds. [21] Investigated the temperature distribution of a wet cylinder liner in a V-12 engine. The study reported FEM predictions that corresponded closely to the experimental outcomes by combining experimental data with finite-element modeling; the largest relative error was only 5.49%. Based on this significant correlation, the study concluded that the theoretical model was quite accurate in predicting the temperature distribution in cylinder liners under various engine thermal-load scenarios [22]. Heat transmission in

Received: 05/06/2026; Revised: 20/07/2026; Accepted: 30/07/2026; Published: 14/08/2026

an aluminum alloy engine piston was investigated experimentally and numerically [23]. The aluminum component's temperature field under high-temperature, combustion-related thermal stress was measured using thermocouples. The study demonstrated that the interaction of high-temperature heat input, conduction through the material and cooling conditions leads to temperature dispersion in aluminum engine components. It also validates the usefulness of taking temperature readings at various points within an engine component and comparing the results to calculate thermal predictions. The study is innovative in that it directly validates the radial temperature distribution predicted by a thermal model while experimentally reproducing the primary thermal boundary conditions of an engine cylinder in a controlled and repeatable laboratory environment. Without the complications of full-scale engine running, this offers a straightforward and economical method for studying steady-state radial heat transfer through engine-cylinder walls.

[17, 24] identified a 10–15% discrepancy between FEA predictions and experimental piston temperatures, attributing this to oversimplified convective boundary conditions at the piston-cylinder interface.. For instance, radial conduction in a cylinder liner, governed by Fourier's law in cylindrical coordinates in the Laplace equation for radial heat conduction is expressed as in equation 1 [25,26. 27]. The steady state condition in the cylinder will tend equation 1 to be zero. It means that at this state the temperature distribution doesn't change with time.

$$\frac{1.d}{r.dr}\left(r\frac{dT}{dr}\right) = 0 \quad (1)$$

The solution for equation 1 call for double integration to yield the temperature distribution in equation2

$$T(r) = C_1 \ln r + C_2 \quad (2)$$

The constants in equation 2 above (C_1, C_2) are determined by the boundary conditions. The solution is a logarithmic function of r. The introduction of boundary conditions to the cylinder will alter the equation 2 above as it appears to be a heat conduction equation without heat generation [28.29]. Taking the inner walls of the cylinder to have a radius as r_1 alongside temperature T_1 . The corresponding external wall with have the outer radius and temperature as r_0, T_0 respectively. Inserting the boundary conditions in equation 2 yields equations 3 and 4.

$$T_1 = C_1 \ln r_1 + C_2 \quad (3)$$

$$T_0 = C_1 \ln r_0 + C_2 \quad (4)$$

The solution lies in the determination of the constant C_1 as seen in equation 5

$$C_1 = \frac{T_1 - T_0}{\ln\frac{r_1}{r_0}} \quad (5)$$

Substituting equation 5 into equation 4 yields the temperature distribution in equation 6

$$T(r) = \frac{(T_1 - T_0)}{\ln\frac{r_1}{r_0}} \ln r + T_1 - \frac{(T_1 - T_0)}{\ln\frac{r_1}{r_0}} \ln r_1 \quad (6)$$

Simplifying equation 6 gives equation 7

$$T(r) = T_1 + \frac{(T_1 - T_0)}{\ln\frac{r_0}{r_1}} . \ln\frac{r}{r_1} \quad (7)$$

Also the heat flux q can be computed using the Fourier law. Knowing that the heat flows uniformly across the cylinder walls and the mode of transfer is conduction. The geometry of the cylinder must be considered [30]. The rate of heat transfer across the cylinder is as expressed in terms of flux according to Fourier law in equation 8

$$q = -k\frac{dT}{dr} = \quad (8)$$

Where q^n the heat flux in w/m2 and k is the thermal conductivity.

Heat transfer Q =qA (9)

Where A is the surface area, assigning A=$2\pi rL$ and solving the mathematical relations yields equation 10. The heat distribution across the cylinder wall at all point is constant

$$Q = 2\pi KL \frac{T_1 - T_0)}{\ln{}^{r_0}/_{r_1}} \quad (10)$$

The heat transfer at the outer surface of the cylinder is a convective mode [31] Employing the Newton law of cooling will help determine the heat transfer coefficient h.

$$h = \frac{Q}{AdT} \quad (11)$$

where dT is the change in temperature ($T_{outer\ wall}$ - $T_{coolenat\ temperature}$)

2.0 Methodology

The experiment used an aluminum cylinder (6061-T6 alloy) from a 2006 model Toyota Camry's 2AZ-FE 2.4L engine, sourced from an automobile workshop in Agbor shown in figure 1. The cylinder outer diameter was 107.58mm, and its length was 98 mm. First, the inner and outer surfaces were cleaned with sandpaper to remove

Received: 05/06/2026; Revised: 20/07/2026; Accepted: 30/07/2026; Published: 14/08/2026

oxidation and debris. Digital vernier calipers were used to confirm the cylinder's dimensions. Small 1 mm holes were drilled radially (inner wall, mid-wall, and outer wall) using a drill press as shown in Figure 2. The preparations were done at the faculty of Engineering workshop, University of Delta, Agbor.

The prepared cylinder was moved to the thermodynamics laboratory at the Department of Mechanical Engineering, University of Delta, Agbor. The K-type thermocouples with a Class 1 accuracy of ±1.5°C or ±0.4% were inserted into these holes and secured with high-temperature epoxy. A cylindrical 1.5kW electric resistance heater which matches the cylinder bore was placed inside the cylinder inner bore to simulate combustion heat. The heater was set to 450°C and controlled by a temperature regulator to maintain steady-state conditions. To prevent heat from escaping axially (top/bottom), ceramic insulation was wrapped around the cylinder's ends, forcing heat to flow radially outward.

A water jacket system was fitted around the cylinder outer surface, with water maintained at 90°C (preheated and circulated via a pump) to replicate engine coolant conditions. The experimental technique used in this investigation is in line with common practice and strictly adheres to the strategy reported by [32]. The heater was turned on until the temperature in the inner wall reached 450°C. The water jacket pump was triggered to keep the coolant flow at 90°C. Thermocouple measurements were observed to have varied by less than ±1°C for ten minutes after the system had been allowed to settle for thirty minutes.

Figure 3 depicts a six-channel digital data recorder that can monitor temperature with a precision of 0.1°C and an accuracy of ±1.5°C using Type-K thermocouples. Every five seconds, temperatures from all thermocouples were recorded within the range of 200 to 1,372°C. Thermocouple measurements validation was achieved using the infrared camera scanning the outside for temperature distribution.. Data was exported after stabilization and compared to ANSYS simulation results to ensure alignment


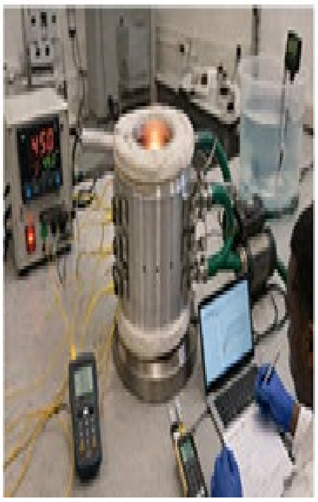

Figure 1. Aluminum cylinder Figure 2: Cylinder preparation Fig.3: Experimental setup

2.1 Modeling and Simulation of Engine Cylinder

A 3D aluminum alloy cylinder was developed using state thermal finite element Analysis. The geometrical values of 43.79 mm inner radius, 53.79 mm outer radius, and 98 mm axial length were used to model the cylinder geometry. The model was given the thermal characteristics of Aluminum Alloy 6061-T6, which include a density of 2700 kg/m³, a specific heat capacity of 896 J/kgK, and a thermal conductivity of 167 W/mK.as shown in Table 1.

A three-dimensional finite-element mesh was used to discretize the cylindrical domain. To effectively capture the radial temperature differential, mesh refinement was applied across the cylinder wall. The experimentally established thermal boundary conditions were then applied to a steady-state thermal analysis. The outside surface was exposed to the cooling condition, which corresponds to a coolant temperature of 90°C and a heat-transfer coefficient of 1100 W/m²K, while the inner cylindrical surface was kept at 450°C, reflecting the high-temperature combustion-side condition. The corresponding reference condition for model validation was the outer-wall temperature of 158°C as determined by experiment. The program-controlled thermal finite element solver was used to derive the thermal solution. The solver was left running until the temperature field reached numerical stability. After convergence, radial positions corresponding to the experimental data points were used to extract the temperature distribution throughout the cylinder wall.

Table 1: Manufacturer data and Model Parameters

Parameters	Values	Parameters	Values
Outer radius	53.79 mm,	Thermal conductivity:	167 W/m·K.
Length	98 mm	Specific heat:	896 J/kg·K.
Inner Bore	43.79mm	Density	2700 kg/m³.
inner wall	1mm	Temperature Boundary Condition T_1	450°C
mid-wall	5mm	Heat Transfer Coefficient h	1100 W/m²·K
outer wall from the inner radius	7.5mm	Coolant temperature	90°C
Cylinder material	AA 6061-T6	Outer wall Temperature T_2	158°C
Compression Ratio	9.6:1	Engine Specifications	2AZ-FE Toyota Camry 2006

3.0 Results and Discussion

3.1 Temperature Gradient across the Cylinder Wall

The temperature readings from thermocouples in Table 2 show radial heat transfer through the cylinder wall from the inner high-temperature combustion zone to the outer cooling water jacket. The significant temperature drop from 418.4°C at the inner thermocouple to 158°C at the outer surface is attributed to conduction and convection. Thermocouple measurements have been used in similar experimental studies of engine-cylinder thermal behavior to assess heat transfer and thermal loading in water-cooled engines as well as cylinder-wall temperature distributions. The logarithmic temperature distribution predicted for radial heat conduction in cylindrical structures, which is derived from Fourier's law in cylindrical coordinates, is in accordance with the observed non-linear temperature gradient. The radial cylindrical shape, heat flow, the cylinder material's thermal conductivity, and the applied thermal boundary conditions combine synergistically to control the temperature fluctuation throughout the cylinder wall. In this sense, the thermal behavior is in line with aluminum 6061-T6's relatively high thermal conductivity, which is often claimed to be between 150 and 170 W/m·K [34,35]

Thermocouple 1T1, positioned 1 mm from the inner wall near the combustion zone, recorded a temperature of 418.4°C, which is slightly lower than the inner wall's combustion temperature of 450°C. This has been reported as heat losses due to conduction. [36].

Inserted thermocouple IT2 (5 mm from inner wall) located midway between inner and outer walls showed a temperature reading of 297.3°C. Temperature drops by 121.1°C over 4 mm, indicating rapid heat dissipation near the inner region. This sharp gradient is due to the smaller radius at this location, where the conductive area is smaller thereby concentrating heat flux. IT3 (7.5 mm from inner wall) placed close to the outer surface recorded 226.2°C having a temperature drops by 71.1°C at a distance of 2.5 mm. At the outer surface, temperature drops by 68.2°C over the final 2.5 mm due to convective cooling by the water jacket. The difference between T_2 (158°C) and the coolant temperature (90°C) reflects the convective thermal resistance in equation 11. Cooling System temperature (90°C) actively maintained by the water jacket to prevent overheating. The large drop from T2 (158°C) to coolant (90°C) suggests moderate convective efficiency. The slight temperature differential between the high-temperature inner zone and the inner cylinder-wall measurement demonstrates a low thermal resistance at the inner surface.

This development is in agreement with the findings of [37.38] who reported that temperature distributions across engine cylinder walls may be employed to determine heat flux, thermal resistance, and heat-transfer behavior. In the current research, the temperature difference between the observed inner-wall temperature and the corresponding high-temperature area indicates the level of thermal resistance associated with heat transmission at the inner surface. Furthermore, the temperature fluctuation across the cylinder wall represents both conduction through the cylindrical material and convective heat transfer to the cooling medium. As a result, the observed temperature distribution is consistent with conventional approaches that employ temperature differences across engine-cylinder walls to evaluate thermal resistance and heat transmission. The steady state heat transfer rate Q through the cylinder was calculated be 147KW using Equation 10 and the convective heat transfer h was equally calculated using equation 11 to be 1100W/m²K.

Table 2: Experimental Measured Temperature at various Radial Positions

Radial Position r (mm)	Radial distance from inner cylinder wall	Measured Temperature (^{0}C)
43.79	0.000	450
	1mm (Inserted Thermocouple (1T1)	418.4
45.79	2.0mm	385.7
47.79	4.0 mm	327.4
	5mm (Inserted Thermocouple(1T2)	297.3
49.79	6.0mm	267.93
	7.5mm (Inserted Thermocouple(1T3)	226.2
51.79	8.0mm	211.70
53.79	10.00mm (Outer Cylinder, T_2)	158
	Coolant Temperature	90
	Ambient Temperature	25

3.2 Mesh Convergence of the Models

The mesh convergence investigation was carried out by gradually refining the finite element mesh shown in figure 4 while observing the predicted temperature at a radial distance of 44.79 mm from the cylinder center. As demonstrated in Figure 5 the predicted temperature changes dramatically with coarser meshes but becomes more stable as the number of elements grows. The coarsest mesh, made up of 5,850 elements with a size of 4.0 mm (Figure 4D), predicted a temperature of 389.54 °C. Increasing the mesh density to 7,560 elements with a size of 3.5 mm (Figure 4C),) resulted in a significant rise in predicted temperature to 395.04°C. Further refining to 14,091 and 20,360 elements, with element diameters of 3.0 mm and 2.5 mm, (Figure 4A and B) respectively, resulted in temperatures of 418.35 °C and 418.48 °C. This indicates that the two finest meshes differ in temperature by just 0.13 °C, or around 0.03%. This little variation shows that the solution is now practically independent on further mesh refinement.

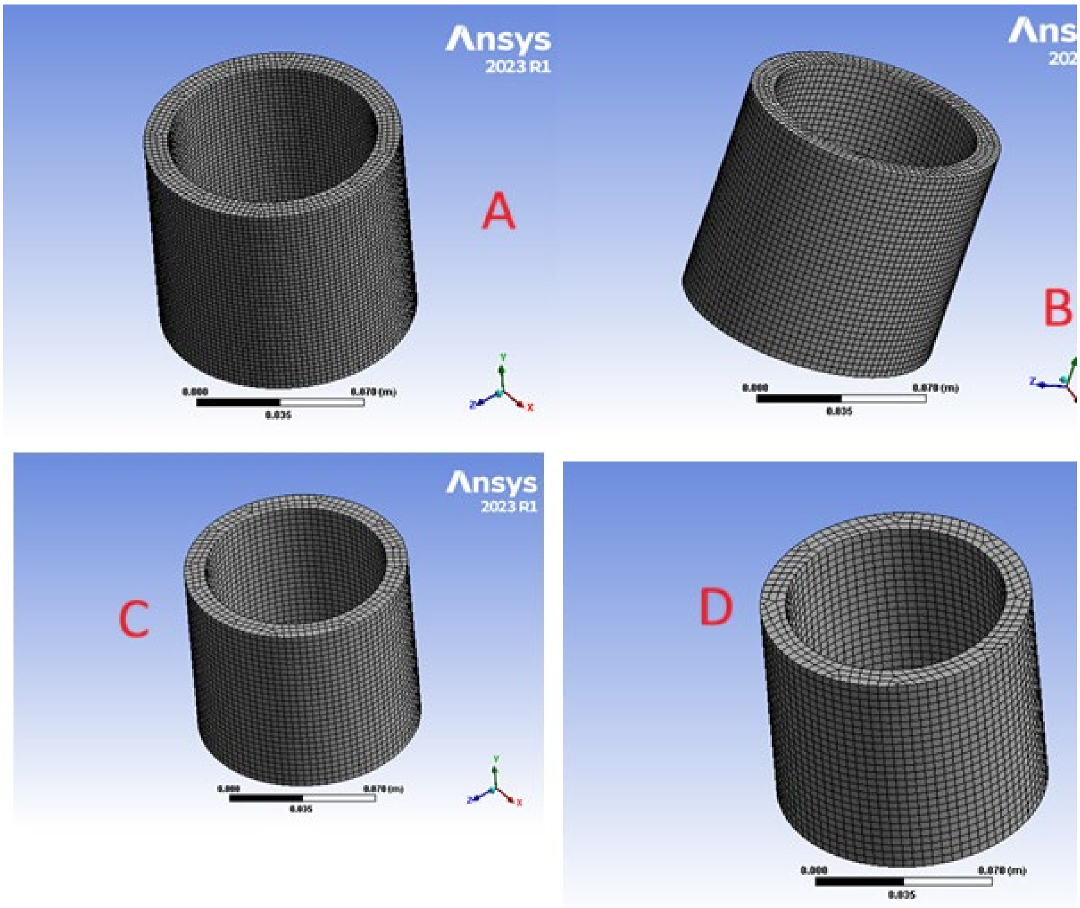

Figure 4: Cylinder meshing

However, difference exists across the various meshes for the temperature readings at 48.79 mm and 51.29 mm, especially for the coarser discretization. The predicted temperature varies from 281.33 °C to 309.15 °C at 48.79

Received: 05/06/2026; Revised: 20/07/2026; Accepted: 30/07/2026; Published: 14/08/2026

mm and from 191.87 °C to 228.89 °C at 51.29 mm. This suggests that the temperature field across the cylinder wall is not sufficiently addressed by the coarser meshes. However, the findings obtained with the two finest meshes demonstrate better agreement, especially at the convergence assessment's monitored position. The convergence trend in Figure 5 also reveals that as the number of mesh elements rises, the solution gets closer to a stable temperature of around 418 °C. The 14,091-element and 20,360-element meshes relatively small rise in temperature from 418.35 °C to 418.48 °C demonstrates that a further mesh refinement barely alters the numerical solution shown also n Table 3. Consequently, the 20,360-element mesh with 97,973 nodes appeared to be completely refined for the thermal investigation. As a result, the mesh was chosen as the best computational mesh since it offers a converged solution without incurring needless computational expenses related to excessive mesh refining.

Table 3: Mesh convergence for the model

Element size (mm)	No. of elements	No. of nodes	Temperature (^{0}C) readings at radial distance		
			44.79 mm	48.79 mm	51.29 mm
2.5	20360	97973	418.48	309.15	228.89
3.0	14091	67644	418.35	297.12	226.95
3.5	7560	38446	395.04	281.33	209.67
4.0	5850	30108	389.54	288.40	191.87

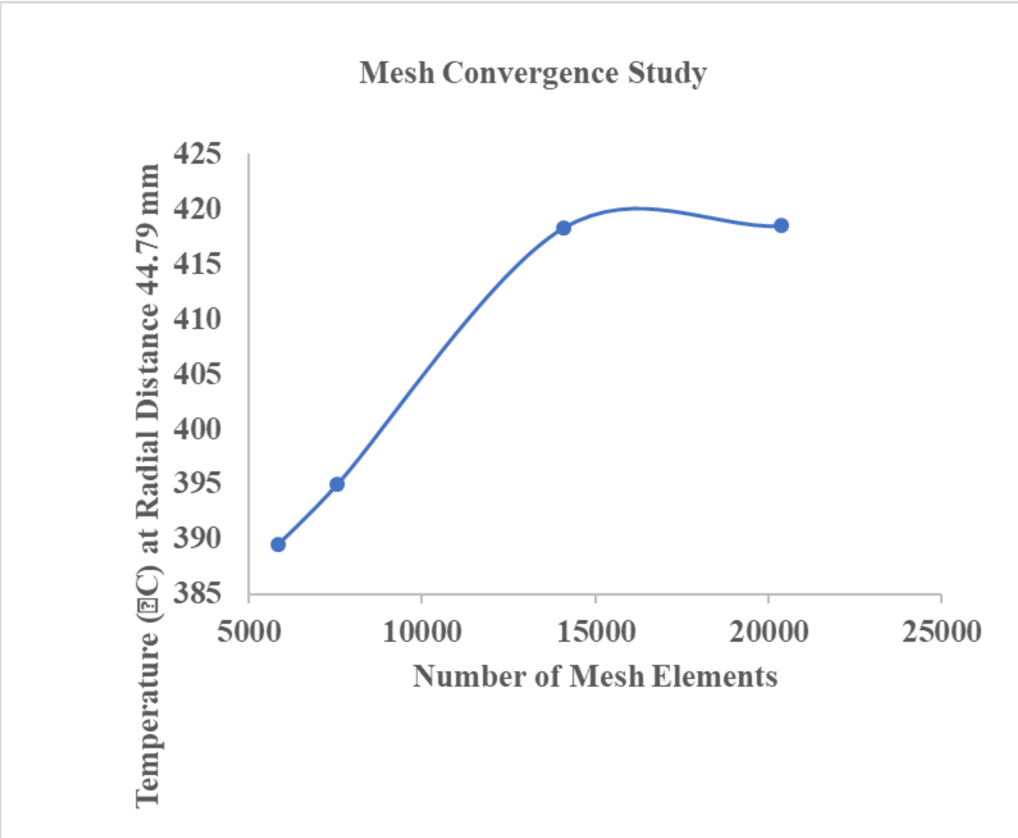

Figure 5: Mesh convergence and independent study for the model

3.3 Thermal Boundary conditions and Temperature readings at radial distances

The engine-cylinder model thermal boundary conditions were developed to approximate the cooling impact on the real-time cylinder wall and the high-temperature interior environment. Figure 6 illustrates the high-temperature combustion-side boundary, a temperature threshold of 450 °C was applied to the inner cylindrical surface. The cooling medium absorbed heat from the cylinder wall using a convective heat-transfer coefficient of 1100 W/m²•°C, and the cooled boundary condition was determined by an outer-wall temperature of 158 °C. A gradual radial temperature decrease from the inner wall toward the outside wall was influenced by the established thermal conditions, which produced a temperature differential of 292 °C between the inner and outer surfaces. An elevated radial thermal gradient is confirmed by the predicted temperatures of 418.48, 309.15, and 228.89 °C for radial distances of 44.79, 48.79, and 51.29 mm, respectively as seen in figure 6. The ANSYS steady-state thermal formulation, which supports specified temperature and convection loads for analyzing temperature fields, thermal gradients, and heat-flow behavior in components subjected to steady thermal loading, is consistent with the

Received: 05/06/2026; Revised: 20/07/2026; Accepted: 30/07/2026; Published: 14/08/2026

corresponding applicable boundary-condition technique. As a result, the basic thermal behavior of a cylinder subjected to both external cooling and a high-temperature interior environment is well represented by the ANSYS model. The temperature contour is in line with how an engine cylinder is designed to function, where heat is transmitted from the combustion wall to the cooling system across the cylinder.

The steady-state thermal study showed that the temperature gradually dropped across the engine cylinder wall's radial thickness. The cooled exterior surface attained the lowest temperature of 158 °C, while the inner wall reached the highest temperature of 450 °C, which satisfied the imposed combustion-side thermal boundary requirement. The predicted temperatures were 418.48, 309.15, and 228.89 °C at radial locations of 44.79, 48.79, and 51.29 mm, respectively. The steady reduction in temperature with increasing radial distance shows the presence of a large radial thermal gradient and suggests that heat is transferred from the inner hot surface to the outside cooled surface. This behavior is consistent with the established thermal behavior of engine cylinder liners reported by [21] who established that heat transfer from the combustion walls through the liner is controlled by heat removal by the cooling medium. The verified numerical engine-wall heat-transfer model developed by [39] likewise shows similar agreement with the current temperature field. As a result, the resulting steady-state thermal model is supported by the ANSYS temperature distribution, which is regarded as physically accurate.

Based on the ANSYS thermal simulation in Figure 6, the engine cylinder steady-state temperature distribution reveals a radial temperature gradient across the cylinder wall, characteristic of internally heated cylindrical components facing external cooling [40]. The highest temperature, approximately 450 °C, occurs at the inner surface where combustion gases directly contact the material. According to [41], the consistent red contour at the bore demonstrates satisfactory application of the internal wall temperature boundary condition. According to the Fourier equation of heat conduction for cylindrical coordinates, the temperature drops radially from the inner bore to the outside wall [42, 43]. The exterior surface temperature of 158 °C is driven by convective heat coefficient of 1100 W/m^2•K and a coolant temperature of 90 °C. This is in tandem with the research outcome of [444] on conventional liquid-cooled internal combustion engine systems, which focus on the role of the cooling mechanism in ensuring stable temperature and heat transmission. The lack of sudden temperature variations over the wall thickness indicates that thermal contact resistance is minimal and that the mesh resolution is sufficient to correctly represent the temperature gradient, as recommended in finite element thermal simulations [45].In general, the temperature field reveals a steady-state equilibrium between external convective heat removal, radial conduction through the cylinder wall, and internal heat input from the combustion process. These findings reflect the report by [46] on engine cylinder thermal design by demonstrating that, despite significant thermal loads on the inner wall, the temperature of the exterior wall remained within acceptable limits, thus minimizing the possibility of material deterioration and thermally induced failure while the engine is operating.

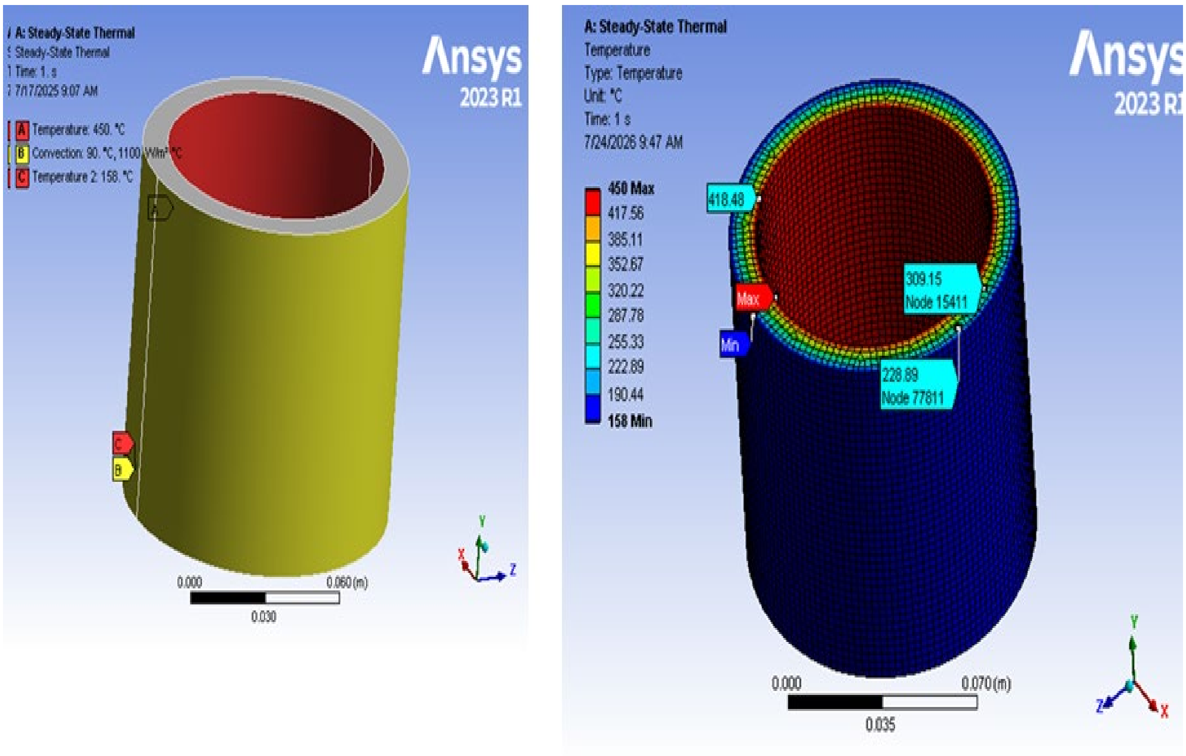

Figure 6: Thermal boundary conditions and simulated Temperature readings at radial distances.

3.4 Comparison of Simulated and Experimental Radial Temperature Distribution

Steady-state conductive heat transmission through the cylindrical thickness is confirmed by the experimentally observed temperatures across the cylinder wall showing a monotonic radial drop from 450 °C at 43.79 mm (inner wall) to 158 °C at 53.79 mm (outer wall). The same basic conductive behavior predicted in hollow cylinders controlled by Fourier's law of heat conduction is also shown by the ANSYS steady-state simulation, which predicts continuous radial temperature decrease. It is essential to note that the experimental and simulated temperatures were not extracted at precisely the same radial positions throughout the cylinder thickness

The experimental data were linearly interpolated at the precise simulated radial distances of 44.79 mm, 48.79 mm, and 51.29 mm in order to guarantee an accurate comparison between the ANSYS-simulated and empirically recorded temperatures, as shown in table 4. The use of this technique allows a straightforward validation of the numerical model. There is only a 0.50 °C difference between the interpolated experimental temperature of 417.85 °C and the simulated temperature of 418.35 °C at 44.79 mm.

The simulation precisely captures substantial thermal loading and radial heat-conduction phenomena as evident by a small deviation. The interpolated actual value (297.665 °C) differs by 11.48 °C from the predicted temperature (309.15 °C) at the 48.79 mm radial point. This shows that the cylinder at mid wall retained more heat Similarly, the computed temperature of 228.89 °C and the interpolated experimental temperature of 225.76 °C at 51.29 mm at the cylinder outer wall differ by just 3.13 °C. This little difference implies that the numerical models properly predicts the rate of conductive heat loss over the cylinder's thickness [47] and precisely reproduce the radial temperature gradient seen in the experiments.

Table 4: Simulated and Experimental Temperatures

Radial distance(mm)	Simulated Temperature(°C)	Interpolated Experimental Temperatures(°C)	Point Errors in Temperature(°C)
44.79	418.35	417.85	0.50
48.79	309.15	297.665	11.48
51.29	228.89	225.7575	3.13

3.5 Statistical Validation of Simulated and Experimental Temperatures at Identical Radial Positions

The numerical model was validated by comparing computed temperatures to interpolated experimental findings at radial distances of 44.79, 48.79, and 51.29 mm. The results show a coefficient of determination (R^2) of 0.9925, RMSE of 6.8791 °C, and MAE of 5.0392 °C, indicating a substantial relation between the simulated and experimental temperature distributions. The relatively high R^2 value, together with the low MAE and RMSE, indicates that numerical projections closely fitted to the radial temperature distribution. A significant difference of 11.485 °C at 48.79 mm shows the highest error, detected, which remains within the allowed range of 15% as stated in prior investigations [17, 24]. The statistical validation ensures its dependability in estimating steady-state temperature distributions in engine cylinders [48, 49]. As a consequence, the model may be utilized confidently for thermal analysis [50].

3.6 Comparison of Simulated and Experimental Heat-Transfer Parameters

Figure 7 shows the engine cylinder wall's radial heat-transfer arrangement. The inner bore surface has the largest thermal gradient (5.42×10^2 W/m²) caused by the presence of high-temperature gases. This is consistent with conventional conduction theory [51], which predicts low material resistance and rapid temperature gradients. The smooth contour bands indicate successful steady-state conduction with established boundary conditions and sufficient numerical mesh resolution. The change from red and yellow to green and blue signifies a reduction in heat transfer towards the outer wall. [52]

The combustion surface heat flux is 5.42×10^2 W/m², resulting in a calculated heat-transfer rate of 146 kW based on an effective area of 0.02695 m² from the cylinder dimensions using Equation 9. The substantial thermal loading and considerable radial temperature gradients in internal combustion engine cylinders that improve conductive heat transfer are highlighted by the quantity of thermal energy that is transported through the cylinder wall during steady-state operation.

The simulated heat-transfer rate of 146 kW differs from the experimental value of 147 kW by just 0.68%, indicating a significant relationship between the computed and experimental heat-transfer characteristics as shown in Table 5. Additionally, the convective heat-transfer coefficient calculation shows that the estimated value of 1080 W/m²•K and the experimental result of 1100 W/m²•K differ by a negligible 1.8%. These minor differences demonstrate a high degree of conformity between numerical predictions and theoretical calculation using the experimental data. Thus, establishing the accuracy of finite-element thermal models in depicting heat-transfer processes.

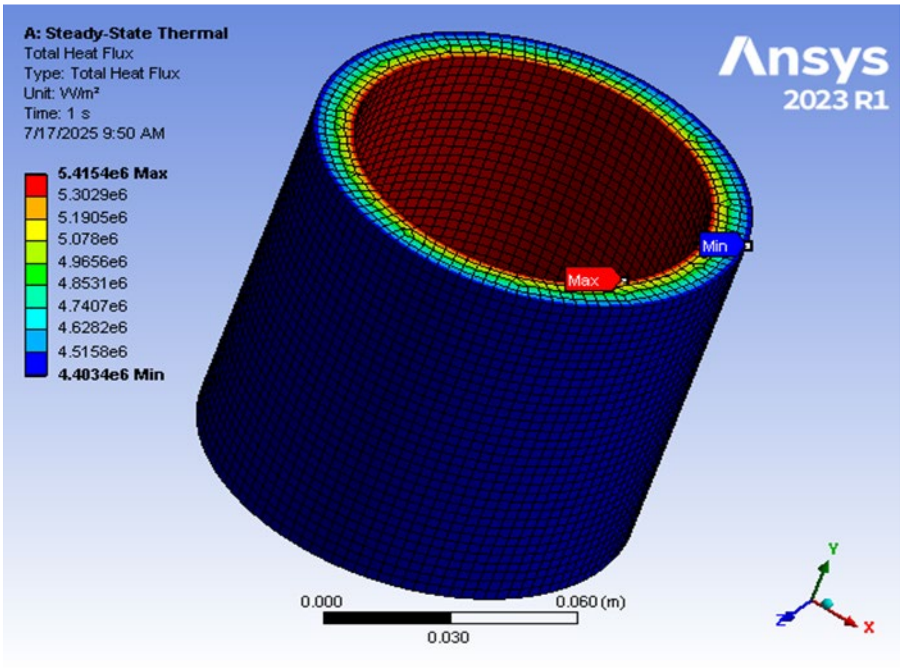

Figure 7: Total heat flux distribution in the model

Table 5: Simulated and Experimental Heat-transfer Parameters

Simulated Parameters	Simulated Values	Experimental Values	% Difference
Heat Transfer rate, Q	146KW	147KW	0.68
Convective Heat-transfer Coefficient, h	1080W/m²	1100 W/m²	1.8

4.0 Conclusion

The work presents a full computational and experimental characterization of steady-state heat transfer in internal combustion engine cylinders.This was achieved by integrating radial temperature measurements and heat flux prediction. The temperature progressively dropped from 450 °C at the combustion surface to 158 °C at a radial distance of 10 mm, according to the experimental results, demonstrating a strong radial thermal gradient that control conductive heat transport mechanism through the cylinder wall.

Radial distances of 44.79 mm, 48.79 mm, and 51.29 mm were recorded, with temperature fluctuations of 0.50 °C, 11.48 °C, and 3.13 °C, indicating a significant convergence between modeling and experimental. The temperature field corresponded to a maximum heat flux of 5.42×10^2 W/m². The experimental heat flux of 147 kW and the predicted value of 146 kW were also nearly matching. The calculated and experimental convective heat-transfer coefficients (1080 W/m²•K and 1100 W/m²•K, respectively) matched well. The validation reveals a small variance of 1.8% for the convective coefficient and 0.68% for heat transfer rates, all of which are below acceptable uncertainty bounds. This research promotes improvements in cooling system design, heat transfer prediction, engine longevity, and efficiency.

References

[1] Torres D.J.G.,Mendes A.S, and Albuquerque C.(2024).Performance and emissions data of an internal combustion engine operating with different ethanol/water mixtures and compression ratios. Data Brief. Vol. 54. https://doi.org/10.1016/j.dib.2024.110390.

[2] Thiagarajan,C. Prabhahar, M, Prakash,S., Senthil,J., Saravana Kumar, M.(2020). Heat transfer Analysis and Optimization of Engine Cylinder Liner using different materials. Materials Today: Proceedings, Volume 33, Part 1, Pages 778-783 https://doi.org/10.1016/j.matpr.2020.06.173

[3] Shinde, S. T., Borole, K. R., Chaudhary, K., & Shinde, N. (2025). Experimental investigation of cylinder liners and performance optimization using ANN. MethodsX,/15,103426. https://doi.org/10.1016/j.mex.2025.103426

[4] Heywood, J. B. (2018). *Internal combustion engine fundamentals* (2nd ed.). McGraw-Hill Education.

[5] Incropera, F. P., DeWitt, D. P., Bergman, T., and Lavine, A. S. (2017). *Fundamentals of heat and mass transfer* (8th ed.). Wiley.

[6] Paul, E., Kevin,D., Cole, D (2002). Fast-converging steady-state heat conduction in a rectangular parallelepiped, International Journal of Heat and Mass Transfer, Volume 45, Issue 17, Pages 3585-3596,

[7] Haji-Sheikh, A., Beck, J.V., Agonafer D, (2003). Steady-state heat conduction in multi-layer bodies. International Journal of Heat and Mass Transfer, Volume 46, Issue 13, Pages 2363-2379,

[8] Yunus A., Çengel, Y. A., Afshin, J., Ghajar, A. J. (2020). *Heat and mass transfer: Fundamentals and applications* (6th ed.). McGraw-Hill Education.

[9] Zhou, H., Ma, P., Cheng, M., and Zhou, M. (2018). Effects of temperature and circulating flue gas components on combustion and NOx emissions characteristics. *ISIJ International, 58*(9), pp1650–1658. https://doi.org/10.2355/isijinternational.ISIJINT-2018-185

[10] Rolf D. R. and Ganesh D (2015). Review of high efficiency and clean reactivity controlled compression ignition (RCCI) combustion in internal combustion engines, Progress in Energyand Combustion Science, Volume 46, Pages12-71, https://doi.org/10.1016/j.pecs.2014.05.003.

[11] Zhan, Z., Fang, B., Wan, S., Bai, Y., Hong, J., and Li, X. (2024). An accurate and efficient implicit thermal network method for the steady-state temperature field. *Proceedings of the Institution of Mechanical Engineers, Part C: Journal of Mechanical Engineering Science.*https://doi.org/10.1177/09544062231187791

[12] Bhagat, A. R and Jibhakate, Y. M.(2012). Thermal Analysis and Optimization of I.C. Engine Piston Using Finite Element Method. International Journal of Modern Engineering Research Vol.2, Issue.4, pp.2919-2921.

[13] Bergman, T. L., Lavine, A. S., Incropera, F. P., and DeWitt, D. P. (2020). Steady-state versus transient methods in heat transfer analysis. Journal of Heat Transfer, 142(4), 040801.

[14] Najibi, A., and Wang, G.H. (2023). Two-Dimensional C-V Heat Conduction Investigation of an FG Finite Axisymmetric Hollow Cylinder.Symmetry,15(5),1009. https://doi.org/10.3390/sym15051009

[15] Alfaris, L., Siagian, R.G., Muhammad, A.C., Nyuswantoro, U.I., and Nasution, B (2023). Heat Conduction in Cylindrical Coordinates with Time-Varying Conduction Coefficients: A Practical Engineering Approach. Journal of Mechanical Engineering Science and Technology (JMEST)*:* Vol. 7: No. 2. https://citeus.um.ac.id/jmest/vol7/iss2/7

[16] Liu, Y., Mitsutake, Y., and Lee, J. (2024). Analytical solution to the two-dimensional inverse heat conduction problem in an axisymmetric cylindrical coordinate system. *International Journal of Thermal Sciences*, 206, 109335. https://doi.org/10.1016/j.ijthermalsci.2024.109335

[17] Motwani R, Gandolfo J, Gainey B, Filipi Z, Lawler B(2024). A 3D CFD-FEA co-simulation study of low thermal effusivity TBCs applied to the piston and valves of an SI engine. *International Journal of Engine Research*. 25(12):2142-2162. doi:10.1177/14680874241265759

[18] Zhang, B., Ma, X., Lu, X., Song, Y., Shi, Y., & Fu, Y. (2023). Effect of cylinder liner cast iron microstructure on friction and wear process. *Materials Science and Technology*, 39(4), 456-468. https://doi.org/10.1080/02670836.2022.2130519

[19] Broatch, P., Olmeda, X., Margot, J. Escalona, A(2019).New approach to study the heat transfer in internal combustion engines by 3D modelling, International Journal of Thermal Sciences, Volume 138, 405-415, https://doi.org/10.1016/j.ijthermalsci.2019.01.006.

[20] Rakopoulos, C. D., Rakopoulos, D. C., Mavropoulos, G. C., & Giakoumis, E. G. (2004). Experimental and theoretical study of the short term response temperature transients in the cylinder walls of a diesel engine at various operating conditions. *Applied Thermal Engineering, 24*(5–6), 679–702. https://doi.org/10.1016/j.applthermaleng.2003.11.002

[21] Trung, K. N. (2021). The temperature distribution of the wet cylinder liner of v-12 engine according to calculation and experiment. *Journal of Thermal Engineering*, *7*(Supp 14), 1872 - 1884. https://doi.org/10.18186/thermal.1051265

[22] Gopujkar, S., Davis, R., Worm, J., Hansley, W., Duncan, J. (2025). Effect of in-cylinder heat transfer and surface temperatures on knock in an SI engine. *International Journal of Engine Research, 26*(10). https://doi.org/10.1177/14680874251319829

[23] Liu, Y., Lei, J., Wang, D., Deng, X., Wen, J., & Wen, Z. (2022). Experimental and simulation study on heat transfer characteristics of aluminium alloy piston under transition conditions. *Scientific Reports, 12*, 9262. https://doi.org/10.1038/s41598-022-13357-0 (Nature)

[24] Cheng, S., Chao, L., Banglin, D., Jing Y., Lili, Z. (2024). Theoretical and numerical investigation of introduced errors in surface temperature measurements of pistons applied in internal combustion engine. Case Studies in Thermal Engineering, Volume 59. https://doi.org/10.1016/j.csite.2024.104441

[25] Tsega, E.G (2022).Numerical Solution of Three-Dimensional Transient Heat Conduction Equation in Cylindrical Coordinates, Journal of Applied Mathematics 1993151, pages 8 https://doi.org/10.1155/2022/1993151

[26] Jalghaf, H. K., Kovács, E., Barna, I. F., & Mátyás, L. (2023). Analytical Solution and Numerical Simulation of Heat Transfer in Cylindrical- and Spherical-Shaped Bodies. Computation, 11(7), 131. https://doi.org/10.3390/computation11070131

[27] Hussain, A., Uddin, M, Haq, S., Jan, Hameed U(2021), Numerical Solution of Heat Equation in Polar Cylindrical Coordinates by the Meshless Method of Lines,.Journal of Mathematics, 8862139, https://doi.org/10.1155/2021/8862139

[28] Das, P., Islam, M. A., Mondal, D., & Nazim, M. S. (2023). Analytical and numerical (FEA) solution for steady-state heat transfer in generic FGM cylinder coated with two layers of isotropic material under convective-radiative boundary conditions. *Heliyon*, *9*(11). e21725

[29] Kayhani,M.H., Norouzi,M., and Amiri D,A.(2012). A general analytical solution for heat conduction in cylindrical multilayer composite laminates. International Journal of Thermal Sciences, Volume 52, Pages 73-82. https://doi.org/10.1016/j.ijthermalsci.2011.09.002

[30] Molla,M.M., Sreebash C., Paul, M.d.,Anwar H,(2009)Natural convection flow from a horizontal circular cylinder with uniform heat flux in presence of heat generation, Applied Mathematical Modeling. Volume33, Issue7, Pp3226-3236, https://doi.org/10.1016/j.apm.2008.10.039

[31] Mohsen,T and Qiao,B.Z (2013)Analytical solution for evaluating the thermal performance and efficiency of convective–radiative straight fins with various profiles and considering all non-linearities. Energy Conversion and Management, Volume 66, Pages 199-210, https://doi.org/10.1016/j.enconman.2012.10.015

[32] Liu, Y., Lei, J and Wang, D. (2022). Experimental and simulation study on heat transfer characteristics of aluminium alloy piston under transition conditions. *Sci Rep* **12**, 9262 https://doi.org/10.1038/s41598-022-13357-0

[33] Jiji, L. M**.** (2009). *Heat Conduction* (3rd ed.). Springer-Verlag Berlin Heidelberg. https://doi.org/10.1007/978-3-642-01267-9

[34] Zhang, A and Li, Y. (2023). Thermal conductivity of aluminum alloys—A review. *Materials, 16*(8), 2972. https://doi.org/10.3390/ma16082972

[35] Mohand S., Khaled L., Mourad B., Mohand T. (2011).Investigation on heat transfer evaluation for a more efficient two-zone combustion model in the case of natural gas SI engines. Applied Thermal Engineering. Volume 31, Issues 2–3, Pages 319. https://doi.org/10.1016/j.applthermaleng.2010.09.012.

[36] Yessaulkov, V., Mitrofanov, A., and Abishev, K. (2024). Numerical analysis of the thermal state of a cylindrical body cooled by an internal fluid flow. Journal of Mechanical Engineering and Sciences, 18(2), 10069-10076. https://doi.org/10.15282/jmes.18.2.2024.8.0795

[37] Carvajal Trujillo, E., Jiménez-Espadafor, F. J., Becerra Villanueva, J. A., & Torres García, M. (2011). Methodology for the estimation of cylinder inner surface temperature in an air-cooled engine. *Applied Thermal Engineering, 31*(8–9), 1474–1481. https://doi.org/10.1016/j.applthermaleng.2011.01.025.

[38] Sharma, S. K., Saini, P. K., & Samria, N. K. (2015). Experimental thermal analysis of diesel engine piston and cylinder wall. *Journal of Engineering, 2015*, Article 178652, 1–10. https://doi.org/10.1155/2015/178652.

[39] Broatch, A., Olmeda, P., Margot, X., & Escalona, J. (2021). Conjugate heat transfer study of the impact of "thermo-swing" coatings on internal combustion engines heat losses. *International Journal of Engine Research*. https://doi.org/10.1177/1468087420960617

[40] Incropera, F. P., DeWitt, D. P., Bergman, T. L. Lavine, A. S. (2020). *Fundamentals of heat and mass transfer* (8th ed.). Wiley

[41] Oghoghorie, O., Ebhojiaye, R. S., and Amiolemhen, P. E. (2022). Thermal and structural analyses of a locally developed internal combustion engine cylinder head using finite element analysis (FEA). *NIPES Journal of Science and Technology Research*, *4*(1), 177–188. DOI:10.37933/nipes/4.1.2022.16

[42] Holman, J. P. (2010). Heat transfer (10th ed.). McGraw-Hill Education.

[43] Zhang, A. and Li, Y. (2023). Thermal Conductivity of Aluminum Alloys—A Review. Materials, 16(8), 2972. https://doi.org/10.3390/ma16082972

[44] Altug, H and Yapici, E. Ö. (2026). Numerical investigation for enhancement of heat transfer in the cooling water jacket of CI engine. Numerical Heat Transfer, Part A: Applications, 87(1). https://doi.org/10.1080/10407782.2025.2541810

[45] ANSYS Inc. (2023). ANSYS Mechanical User's Guide. ANSYS® Release 2023 R1 Documentation (Help System). Canonsburg, PA, USA

[46] Trung, K. N. (2021). Temperature distribution of the wet cylinder liner of v-12 engine according to calculation and experiment. *Journal of Thermal Engineering*, *7*(Supp 14), 1872-1884. https://doi.org/10.18186/thermal.1051265

[47] Yang, L., Lu, G., and Wang, T. (2024). Structure Improvement of Two-Cylinder Engine Cooling Water Jacket Based on Flow Field Simulation. Sustainability,16(24), 11092. https://doi.org/10.3390/su162411092

[48] Chai, T. and Draxler, R. R. (2014) Root mean square error (RMSE) or mean absolute error (MAE). Arguments against avoiding RMSE in the literature, Geosci. Model Dev., 7, 1247–1250, https://doi.org/10.5194/gmd-7-1247-

[49] Willmott, C. J., & Matsuura, K. (2005). Advantages of the mean absolute error (MAE) over the root mean square error (RMSE) in assessing average model performance. *Climate Research, 30*, 79–82
[50] https://doi.org/10.3354/cr030079
[51] Petkov, D., and Iliev, S. (2026). Numerical Modelling of the Thermal State of a Cylinder Head. Engineering Proceedings, 122(1), 13. https://doi.org/10.3390/engproc2026122013
[52] Bergman, T.L., Lavine, S.A., Incropera, F.P. and Dewitt, D.P. (2011) Fundamentals of Heat and Mass Transfer. 7th Edition, John Wiley & Sons, Hoboken.
[53] Agarwal, A., Dinka, M. O and Ilunga, M. (2024). Enhancing Engine Cylinder Heat Dissipation Capacity Through Direct Optimization (DO) Techniques. Processes, 12(12), 2659. https://doi.org/10.3390/pr12122659
[54] Zhang, B., Long, Z., Liu, G., Wu, Z., and Yan, Q. (2025). Investigating the distribution of heat transfer in a thick-walled functionally graded cylindrical shell under heat flux. Journal of Engineering and Applied Science, *72*, 1. https://doi.org/10.1186/s44147-024-00571-y